Received May 31, 2019, accepted June 19, 2019, date of publication June 27, 2019, date of current version July 16, 2019.

Digital Object Identifier 10.1109/ACCESS.2019.2925380

Secrecy Performance Analysis of Relay Selection in Cooperative NOMA Systems

ZHENLING WANG AND ZHANGYOU PENG

Key Laboratory of Specialty Fiber Optics and Optical Access Networks, Shanghai University, Shanghai 200444, China

Corresponding author: Zhangyou Peng (zypeng@mail.shu.edu.cn)

ABSTRACT This paper investigates the security performance of two relay selection schemes for cooperative non-orthogonal multiple access (NOMA) systems, where K randomly distributed relays are employed with either decode-and-forward (DF) or amplify-and-forward (AF) protocols. More particularly, two-stage relay selection (TRS) and optimal relay selection (ORS) schemes are taken into consideration. To characterize the secrecy behaviors of these RS schemes, new closed-form expressions of both exact and asymptotic secrecy outage probability (SOP) are derived. We confirm that the SOP of the TRS scheme is equal to that of the ORS scheme for DF/AF-based NOMA systems. Based on the analytical results, the secrecy diversity orders achieved by the pair of RS schemes for the DF/AF-based NOMA systems are K, which are equal to the number of relays. It is shown that the secrecy diversity orders for the cooperative NOMA systems are determined by the number of the relays. The numerical results are presented to demonstrate that: 1) the secrecy performance of the AF-based NOMA system outperforms that of the DF-based NOMA system, when not all DF relays successfully decode the received information; 2) with the number of relays increasing, the SOP of these RS schemes for the DF-/AF-based NOMA systems becomes lower, and; 3) the TRS/ORS schemes are capable of achieving better secrecy outage behaviors compared with random RS and orthogonal multiple access-based RS schemes.

INDEX TERMS Amplify-and-forward, decode-and-forward, non-orthogonal multiple access, physical layer security, relay selection.

I. INTRODUCTION

With the rapid increase of the wireless capacity requirements imposed by advanced multimedia applications and services, spectral efficiency has been a key factor to support the demands of increased traffic and data throughput in the fifth generation (5G) mobile communication networks. Due to conventional orthogonal multiple access (OMA) encountered bottlenecks in service provisioning, non-orthogonal multiple access (NOMA) has been one of the promising techniques to further improve the network capacity [1], [2]. Different from OMA, the signals of multiple users are linearly superposed [3] in the same physical resource by the different power coefficients. Then successive interference cancellation (SIC) scheme [4], [5] is employed to detect the desired signal. It has been proved that NOMA is able to achieve the superior outage behavior and spectral efficiency than that of OMA [6]–[8]. Apart from enhancing the system performance, NOMA guarantees high fairness requirements of multiple users through appropriate power allocation scheduling [9], [10].

NOMA has been extended to cooperative communications [11], [12], where the users with better channel conditions were selected as decode-and-forward (DF) relays to deliver information and improve transmission reliability of users with poor channel conditions. Inspired by this, the authors of [13] have analyzed the outage performance of DF-based NOMA system with full-duplex (FD) and half-duplex (HD) scenarios, respectively. From the perspective of enhancing spectrum efficiency and energy efficiency, simultaneous wireless information and power transfer has been applied to cooperative NOMA [14], [15], in which the user relays harvest energy from base station (BS). Specifically, in [15], the authors comprehensively analyzed the system performance under considering DF and amplify-and-forward (AF) protocols. On the other hand, cooperative NOMA schemes with dedicated relays have been widely investigated. The cooperative NOMA systems with AF relays are obviously superior to cooperative OMA in terms of coding gain, outage performance and system throughput in [16]–[18].

The associate editor coordinating the review of this manuscript and approving it for publication was Yuanwei Liu.

Additionally, the outage probability and sum rate of the cooperative NOMA system with DF relay have been studied over Nakagami-m fading [19]. Moreover, the authors researched the outage behaviors of downlink NOMA with both DF and AF protocols [20], where partial channel state information was available to determine the decoding order of cell-edge users data. Very recently, to characterize the effects of the hardware impairments and imperfect channel state information brought in the cooperative NOMA networks, the performance of cooperative NOMA systems with the two imperfections have been analyzed [21]–[23] in terms of the outage probability and throughput. Considering the potential performance gain brought by FD cooperative NOMA, the outage probability and ergodic rate of the two-way relay cooperative NOMA system [24] has been investigated.

To further take advantages of space diversity and improve the spectral efficiency, multiple relay selection (RS) scheme has been widely investigated. Full diversity orders were obtained by exploiting signal-to-noise ratio (SNR) optimal and suboptimal multiple RS schemes in [25]. Driven by this, two-stage RS (TRS) strategy was proposed for cooperative NOMA system [26], where the outage performance was characterized. It was shown that the TRS scheme is capable of achieving minimal outage probability and maximal diversity order. On the basis of [26], the authors have investigated the impact of RS on the performance of cooperative NOMA with HD and FD relays, where single-stage RS (SRS) and TRS schemes were considered in detail [27]. Besides, the authors of [28] comprehensively investigated the outage probabilities and diversity orders of the DF and AF NOMA systems with TRS scheme, respectively. In [29], both two-stage weighted-max-min and max-weighted-harmonic-mean schemes were proposed for cooperative NOMA system, where the outage probabilities were analyzed with fixed and adaptive power allocations at the relays, respectively. Furthermore, the system throughput was analyzed in a two-phase NOMA system with RS [30]. It was verified that the system throughput of cooperative NOMA with RS outperforms that of the conventional OMA and non-cooperative NOMA.

As the broadcast nature of wireless transmissions, the concept of physical layer security (PLS) was firstly proposed from the perspective of information theory [31]. Obviously, combining wireless communication and PLS is the research topic which has sparked of wide interest [32], [33]. The secrecy performance has been analyzed in downlink multiuser OMA system and multiuser multirelay network in [32] and [33], respectively. However, the above works are related to OMA system. Very recently, the PLS has extended to the design of NOMA system [34], in which the secrecy outage probability (SOP) was adopted as a evaluation metric. The impact of PLS on the performance of a unified NOMA framework has been investigated under considering both external and internal eavesdropping scenarios [35]. To enhance PLS, the SOP was derived with considering single-antenna and multiple-antenna scenarios, respectively [36]. As a further advance, the joint subcarrier assignment and power allocation problem for two-way relay NOMA system were studied to maximize the achievable secrecy energy efficiency in [37]. Additionally, the authors of [38] investigated the secrecy performance of a downlink NOMA system with suboptimal and optimal antenna selection schemes. To improve the secrecy performance of the NOMA system, a max-min transmit antenna selection strategy was exploited [39], where messages were transmitted from a BS to multiple legitimate destinations and wiretapped by multiple eavesdroppers (Eves). More particularly, the PLS for cooperative NOMA system was researched based on AF and DF protocols in [40]. Furthermore, in [41], the secrecy behaviors of multiple relays NOMA system were characterized with three RS schemes, namely optimal single RS scheme, two-step single RS scheme and optimal dual RS scheme. It is worth noting that the SOP of cooperative NOMA systems with fixed power allocation [40], [41] converges to an error floor and obtains a zero diversity order.

A. MOTIVATION AND CONTRIBUTIONS

While the aforementioned significant contributions have laid a solid foundation for the understanding the PLS and RS techniques, there is still a paucity of research contributions on investigating the security issues of NOMA with RS. By exploiting RS schemes, the requirements of Internet of Things (IoT) scenarios, such as link density, coverage enhancement and small packet service are capable of being fulfilled. In [27], a pair of RS schemes namely SRS scheme and TRS schemes were proposed for FD/HD NOMA systems, where K relays were uniformly distributed over a circular area of a given radius. However, the security issues of NOMA were not considered in [27]. It is important to emphasize PLS in wireless communication systems, since the broadcast nature of wireless transmissions. The authors of [40] have investigated the secrecy performance of cooperative NOMA system, but just one relay with AF or DF protocol was employed to forward the information, i.e., the impact of spatially random RS on the secrecy performance of cooperative NOMA was not analyzed. To the best of our knowledge, there are no existing works to investigate the secrecy performance of cooperative NOMA with RS schemes. Motivated by these, we specifically consider the secrecy performance of the cooperative NOMA system with RS schemes. More particularly, both TRS and optimal RS (ORS) schemes are taken into account in the proposed system. In the TRS scheme, on the condition of ensuring the targeted secrecy data rate of distant user, the nearby user is served with secrecy data rate as large as possible for selecting a relay. In the ORS scheme, one optimal relay is selected for minimize the SOP of the NOMA system. Based on the proposed schemes, the primary contributions can be summarized as follows:

1) We investigate the secrecy outage behaviors of TRS and ORS schemes for DF-based NOMA system, respectively. We further derive the closed-form and asymptotic expressions of SOP for DF-based NOMA RS schemes. The DF-based NOMA RS schemes are

capable of providing the secrecy diversity orders of K, which is equal to the number of relays. We observe that the SOP of the ORS scheme is equal to that of TRS scheme for DF-based NOMA system.

2) We also derive the closed-form expressions of SOP for AF-based NOMA RS schemes. To get further insights, the asymptotic SOP expressions of AF-based NOMA RS schemes are derived. Based on the analytical results, we acquire secrecy diversity orders of the AF-based NOMA RS schemes, which are equal to K. We confirm that the secrecy diversity orders for DF/AF-based NOMA systems are determined by the number of the relays. Moreover, the SOP of the ORS scheme is also equal to that of TRS scheme for AF-based NOMA system.
3) We confirm that the secrecy behavior of AF-based NOMA system outperforms that of DF-based NOMA system, when not all DF relays successfully decode the received information. Furthermore, we observe that the SOP for DF/AF-based NOMA RS schemes becomes lower with the number of relays increasing. Additionally, it is shown that the DF/AF-based NOMA TRS/ORS schemes are able to achieve better secrecy outage performance compare to random RS (RRS) and OMA based RS schemes.

B. ORGANIZATION

The rest of this paper is organized as follows. In Section II, the secure NOMA network model with spatially random RS is presented. In Section III, the RS schemes are described and the secrecy behavior of the system with DF relays is investigated. Furthermore, the secrecy behavior of the system with AF relays is studied based on the proposed RS schemes in section IV. Numerical results are provided for performance evaluation and comparison in Section V. Finally, Section VI concludes the paper.

II. SYSTEM MODEL

In this section, network description and signal model are provided in detail.

A. NETWORK DESCRIPTION

Consider a downlink secure NOMA network including one BS, K relays (R_i with $1 \leq i \leq K$), two legitimate users (LUs), i.e., the nearby user D_1 and distant user D_2, and an Eve, as shown in Fig. 1. Assuming that the BS is located at the origin of a disc D and the radius of the disc is R_D. In addition, K relays are uniformly distributed within D. Without loss of generality, we consider only one Eve[1] and assume that the Eve is located in the vicinity of the LUs (the edge of cell). The Eve is passive all the time and attempts to intercept the information. Due to deep fading, we assume that direct links between BS and the LUs, as well as Eve do not exist. Moreover, the DF and AF protocols are considered at each relay and only one relay is selected to assist BS transmitting information to the LUs. As such, the Eve can only overhear the messages from the relay selected. Furthermore, all relays employ HD mode and all nodes in the network have single antennas. $h_{SR_i} \sim CN(0,1)$, $h_{R_iD_1} \sim CN(0,1)$, $h_{R_iD_2} \sim CN(0,1)$ and $h_{R_iE} \sim CN(0,1)$ denote the complex channel coefficient of $BS \rightarrow R_i$, $R_i \rightarrow D_1$, $R_i \rightarrow D_2$ and $R_i \rightarrow Eve$ links, respectively, which are assumed to be independent non-selective block Rayleigh fading. d_1, d_2 and d_e denote the distance from the BS to D_1, D_2 and Eve, respectively. In NOMA communication systems, users are generally classified into two types by their quality of service (QoS) not sorted by their channel conditions [27], i.e., the nearby users and distant users, where the nearby users require a high date rate and the distant users may only require a predetermined low data rate. More particularly, our proposed system model with the QoS requirements of NOMA users can be applied to IoT scenarios. Hence D_1 can be served opportunistically with a higher targeted secrecy data rate, e.g., to download video files, while D_2 should be served quickly with a lower targeted secrecy data rate, e.g., to send temperature and humidity information containing in a few bytes as an environmental monitoring sensor.

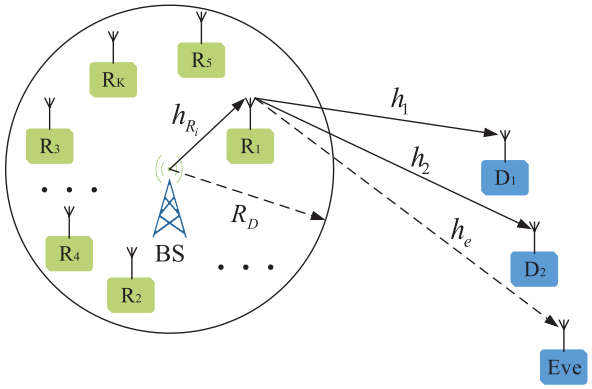

FIGURE 1. An illustration of RS schemes for downlink secure NOMA communication.

B. SIGNAL MODEL

In the first time slot, BS broadcasts the superposed signal $\sqrt{a_1 P_s}x_1 + \sqrt{a_2 P_s}x_2$ to the relay according to NOMA principle, where x_1 and x_2 are the unit power signal for D_1 and D_2, respectively. The corresponding power allocation coefficients of D_1 and D_2 are a_1 and a_2, respectively. Specially, we assume that $a_1 \leq a_2$ with $a_1 + a_2 = 1$ to stipulate better fairness and QoS requirements between the users. Therefore, the received signal at the ith relay R_i can be given by

$$y_{R_i} = h_{R_i}\left(\sqrt{a_1 P_s}x_1 + \sqrt{a_2 P_s}x_2\right) + n_{R_i}, \quad (1)$$

where $h_{R_i} = \frac{h_{SR_i}}{\sqrt{1+d_{SR_i}^{\alpha}}}$, d_{SR_i} denote the distance from the BS to R_i and α denotes the path loss exponent. P_s represents normalized transmission power of BS. n_{R_i} denotes the Gaussian

[1] In this paper, we consider only one Eve for the proposed NOMA system. Multiple Eves scenarios can be developed for further evaluating the secrecy performance of NOMA networks.

noise with zero mean and variance N_0 at R_i. The next part, we explain the transmission process for DF and AF protocols, respectively.

1) DECODE-AND-FORWARD

For DF case, the SIC scheme is first employed at R_i to detect the signal x_2 of D_2. Hence the received signal-to-interference-plus-noise ratio (SINR) at R_i to detect x_2 is given by

$$\gamma_{D_2\to R_i}^{DF} = \frac{\rho|h_{R_i}|^2 a_2}{\rho|h_{R_i}|^2 a_1 + 1}, \tag{2}$$

where $\rho = \frac{P_s}{N_0}$ is transmit SNR of the link between R_i and users. After decoding D_2's message and subtracting it, R_i is further to detect D_1's information with the following SINR

$$\gamma_{D_1\to R_i}^{DF} = \rho|h_{R_i}|^2 a_1. \tag{3}$$

For simplicity, we assume that R_i is capable of decoding the two LUs' information, i.e, satisfying $\frac{1}{2}\log(1+\gamma_{D_1\to R_i}^{DF}) > R_1^{th}$ and $\frac{1}{2}\log(1+\gamma_{D_2\to R_i}^{DF}) > R_2^{th}$, where R_2^{th} and R_2^{th} are the target data rate of D_1 and D_2, respectively. Then in the second time slot, R_i re-encodes and forwards it to $D_j, j \in (1, 2)$. Therefore the received signals at D_j can be given by

$$y_{D_j}^{DF,i} = h_j\left(\sqrt{a_1 P_r}x_1 + \sqrt{a_2 P_r}x_2\right) + n_{D_j}, \tag{4}$$

where $h_j = \frac{h_{R_iD_j}}{\sqrt{1+d_{R_iD_j}^{\alpha}}}$, $d_{R_iD_j}$ denotes the distance from R_i to D_j (assuming $d_{R_iD_j} \gg d_{SR_i}$). $d_{R_iD_j}$ can be expressed as $d_{R_iD_j} = \sqrt{d_{SR_i}^2 + d_j^2 - 2d_j d_{SR_i}\cos(\vartheta_i)}$ and ϑ_i is the angle $\angle SR_iD_j$. P_r represents normalized transmission power of R_i and assuming $P_r = P_s$. n_{D_j} denotes the Gaussian noise with zero mean and variance N_0 at D_j.

Similarly, we assume SIC can be also implemented successfully at D_1, i.e., D_1 first decode and subtract D_2's message x_2, then it further to detect its own information with the following SINR

$$\gamma_{D_1}^{DF,i} = \rho|h_1|^2 a_1. \tag{5}$$

The received SINR at D_2 to detect its own message is given by

$$\gamma_{D_2}^{DF,i} = \frac{\rho|h_2|^2 a_2}{\rho|h_2|^2 a_1 + 1}. \tag{6}$$

With (2), (3), (5) and (6), the achievable capacity of D_j based on DF relaying can be expressed as

$$C_{D_j}^{DF,i} = \frac{1}{2}\log\left\{1 + \min\left(\gamma_{D_j\to R_i}^{DF}, \gamma_{D_j}^{DF,i}\right)\right\}. \tag{7}$$

Meanwhile, as the broadcast nature of wireless transmission, Eve can also receive the signal from R_i. The observation at Eve is given by

$$y_e^{DF,i} = h_e\left(\sqrt{a_1 P_r}x_1 + \sqrt{a_2 P_r}x_2\right) + n_e, \tag{8}$$

where $h_e = \frac{h_{R_iE}}{\sqrt{1+d_{R_iE}^{\alpha}}}$, d_{R_iE} denotes the distance from R_i to Eve (assuming $d_{R_iE} \gg d_{SR_i}$). n_e denotes the Gaussian noise with zero mean and variance N_e at Eve.

In this paper, we suppose that Eve has the multiuser detection capability. In particularly, parallel interference cancellation (PIC) is employed at Eve to decode the superposed signal of LUs. Hence the received SINR at Eve to detect D_j's message can be written as

$$\gamma_{D_j\to E}^{DF,i} = \rho_E|h_e|^2 a_j, \tag{9}$$

where $\rho_E = \frac{P_r}{N_e}$ is the average SNR of the illegal link, i.e., the link between R_i and Eve. The channel capacity from R_i to Eve can be expressed as

$$C_{D_j\to E}^{DF,i} = \frac{1}{2}\log\left(1 + \gamma_{D_j\to E}^{DF,i}\right). \tag{10}$$

Combine (7) and (10), the capacity of D_j in the DF-based NOMA network is given by

$$C_{S,D_j}^{DF,i} = \left[C_{D_j}^{DF,i} - C_{D_j\to E}^{DF,i}\right]^+, \tag{11}$$

where $[x]^+ = \max\{x, 0\}$.

2) AMPLIFY-AND-FORWARD

For AF case, R_i amplifies and forwards its received signals to D_j in the second time slot. Therefore the observation at D_j can be expressed as

$$y_{D_j}^{AF,i} = Gh_{R_i}h_e\left(\sqrt{a_1 P_s}x_1 + \sqrt{a_2 P_s}x_2\right) + Gh_e n_{R_i} + n_e, \tag{12}$$

where $G = \sqrt{\frac{1}{|h_{R_i}|^2 + 1/\rho}}$ is the amplifying factor.

Similar to DF case, we assume that D_1 first decodes x_2 successfully and subtract it. Then the received SINR at D_1 is given by

$$\gamma_{D_1}^{AF,i} = \frac{|h_{R_i}|^2|h_1|^2 a_1 \rho}{|h_1|^2 + |h_{R_i}|^2 + \frac{1}{\rho}}. \tag{13}$$

The received SINR at D_2 to detect its own message in AF case can be given by

$$\gamma_{D_2}^{AF,i} = \frac{|h_{R_i}|^2|h_2|^2 a_2}{|h_{R_i}|^2|h_2|^2 a_1 + \frac{1}{\rho}|h_2|^2 + \frac{1}{\rho}|h_{R_i}|^2 + \frac{1}{\rho^2}}. \tag{14}$$

Based on (13) and (14), the achievable capacity of D_j based on AF relaying can be expressed as

$$C_{D_j}^{AF,i} = \frac{1}{2}\log\left\{1 + \gamma_{D_j}^{AF,i}\right\}. \tag{15}$$

Moreover, Eve can also receive the signal from R_i and the observation at Eve is given by

$$y_e^{AF,i} = Gy_{R_i}h_e + n_e. \tag{16}$$

Since PIC is employed at Eve, in AF case, the received SINR at Eve to detect D_j's message can be written as

$$\gamma_{D_j\to E}^{AF,i}=\frac{|h_{R_i}|^2|h_e|^2a_j\rho\rho_E}{\rho_E|h_e|^2+\rho|h_{R_i}|^2+1}. \tag{17}$$

Similarly, the channel capacity from R_i to Eve can be expressed as

$$C_{D_j\to E}^{AF,i}=\frac{1}{2}\log\left(1+\gamma_{D_j\to E}^{AF,i}\right). \tag{18}$$

With (15) and (18), the capacity for D_j in the AF-based NOMA network is given by

$$C_{S,D_j}^{AF,i}=\left[C_{D_j}^{AF,i}-C_{D_j\to E}^{AF,i}\right]^+. \tag{19}$$

III. SECRECY PERFORMANCE EVALUATION FOR DF-BASED NOMA SYSTEM

In this section, the secrecy behaviors of a pair of RS schemes are characterized in terms of SOP for DF-based NOMA system, which are detailed in the following.

Firstly, the following set of the relays that can correctly decoding the superposed signals [27], [28] can be given as

$$\Theta=\arg_i\left\{\frac{1}{2}\log(1+\gamma_{D_1\to R_i}^{DF})>R_1^{th},\ \frac{1}{2}\log(1+\gamma_{D_2\to R_i}^{DF})>R_2^{th}, i\in S_R\right\}, \tag{20}$$

where S_R denotes the number of the relays in the network, i.e., $S_R=\{1,2,\cdots,K\}$.

Then, a relay is selected from Θ to transmit messages to the users. Hence the SOP of the DF-based NOMA system can be expressed as

$$P_{out}^{DF}=\sum_{m=0}^{K}\Pr(|\Theta|=m)P_{M,\theta_m}^{DF}, \tag{21}$$

where $|\Theta|$ denotes the size of Θ and $M\in(TRS,ORS)$. P_{M,θ_m}^{DF} denotes the SOP of TRS/ORS schemes under the condition that there are m relays that correctly decode the superposed signals.

The probability $\Pr(|\Theta|=m)$ in (21) can be further expressed as (22), as shown at the top of the next page.

Lemma 1: The closed-form expression of $\Pr(|\Theta|=m)$ *in (21) can be approximated as*

$$\begin{aligned}\Pr(|\Theta|=m)=&C_K^m\left[1-\frac{\pi}{2N}\sum_{n=1}^{N}\sqrt{1-\phi_n^2}\left(1-e^{-c_n\tau}\right)\times(\phi_n+1)\right]^m\\&\left[\frac{\pi}{2N}\sum_{n=1}^{N}\sqrt{1-\phi_n^2}\times\left(1-e^{-c_n\tau}\right)(\phi_n+1)\right]^{K-m},\end{aligned} \tag{23}$$

where $\tau=\max\left(\frac{2^{2R_1^{th}}-1}{a_1\rho},\frac{2^{2R_2^{th}}-1}{\left(a_2-\left(a_1 2^{2R_2^{th}}-1\right)\right)\rho}\right)$, $c_n=1+\left(\frac{R_D}{2}(\phi_n+1)\right)^{\alpha}$, $\phi_n=\cos\left(\frac{2n-1}{2N}\pi\right)$ *and* N *is a parameter to ensure a complexity-accuracy tradeoff.*

Proof: See Appendix A. ■

A. TWO-STAGE RELAY SELECTION SCHEME

The TRS scheme main include two stages [27], [28] for the cooperative NOMA system: 1) In the first stage, the targeted secrecy data rate of D_2 is to be satisfied; and 2) In the second stage, on the condition that the secrecy data rate of D_2 is ensured, we serve D_1 with secrecy data rate as large as possible. Hence the first stage activates the relays that satisfy the following condition

$$\Phi=\arg_i\left\{C_{S,D2}^{DF,i}>R_2^S, i\in\Theta\right\}, \tag{24}$$

where R_2^S is the targeted secrecy data rate of D_2. Among the relays in Φ, a relay is selected which can maximize the secrecy data rate of D_1 to convey the information in the second stage, i.e., the relay is selected as the following criterion

$$i_{TRS}^*=\arg_i\max\left\{C_{S,D1}^{DF,i}>R_1^S, i\in\Phi\right\}, \tag{25}$$

where R_1^S is the targeted secrecy data rate of D_1.

According to the proposed TRS scheme, the SOP of the cooperative NOMA system on the condition $|\Theta|=m$ can be given as

$$P_{TRS,\Theta_m}^{DF}=\Pr(\Psi_1)+\Pr(\Psi_2), \tag{26}$$

where Ψ_1 and Ψ_2 are the outage events. Ψ_1 denotes that the relay set Φ is an empty set, i.e., no relay can be selected to satisfy the targeted secrecy data rate of D_2. Ψ_2 denotes i_{TRS}^* is an empty set when Φ is a non-empty set, i.e., no relay can be selected to satisfy the targeted secrecy data rate of D_1 when there exists relays satisfy the targeted secrecy data rate of D_2.

Based on the above analysis, the first outage probability in (26) can be expressed as

$$\Pr(\Psi_1)=\prod_{i=1}^{m}\Pr\left(C_{S,D_2}^{DF,i}<R_2^S\right). \tag{27}$$

Define $C_{S,D_1}^{DF,i_{TRS}^*}=\max\left\{C_{S,D_1}^{DF,k},\forall k\in\Phi\right\}$, we can obtain the out probability $\Pr(\Psi_2)$ as

$$\begin{aligned}\Pr(\Psi_2)&=\sum_{k=1}^{m}\Pr\left(C_{S,D_1}^{DF,i_{TRS}^*}<R_1^S,|\Phi|=k\right)\\&=\sum_{k=1}^{m}\Pr\left(C_{S,D_1}^{DF,i_{TRS}^*}<R_1^S\middle||\Phi|=k\right)\Pr(|\Phi|=k)\\&=\sum_{k=1}^{m}\left[\underbrace{\Pr\left(C_{S,D_1}^{DF,i}<R_1^S\middle||\Phi|=k\right)}_{\psi_1}\right]^k\underbrace{\Pr(|\Phi|=k)}_{\psi_2}.\end{aligned} \tag{28}$$

$$\Pr\left(|\Theta|=m\right)=C_K^m\left(\underbrace{\Pr\left(\frac{1}{2}\log(1+\gamma^{DF}_{D_1\to R_i})>R_1^{th},\frac{1}{2}\log(1+\gamma^{DF}_{D_2\to R_i})>R_2^{th}\right)}_{Q}\right)^m \times\left(1-\Pr\left(\frac{1}{2}\log(1+\gamma^{DF}_{D_1\to R_i})>R_1^{th},\frac{1}{2}\log(1+\gamma^{DF}_{D_2\to R_i})>R_2^{th}\right)\right)^{K-m}. \tag{22}$$

The ψ_1 in (28) can be written as

$$\begin{aligned}\psi_1&=\Pr\left(C^{DF,i}_{S,D_1}<R_1^S\middle|\, i\in\Phi,|\Phi|>0\right)\\&=\Pr\left(C^{DF,i}_{S,D_1}<R_1^S\middle|\, C^{DF,i}_{S,D_2}>R_2^S\right),\end{aligned} \tag{29}$$

according to the definition of conditional probability, ψ_1 can be further expressed as

$$\psi_1=\frac{\Pr\left(C^{DF,i}_{S,D_1}<R_1^S,C^{DF,i}_{S,D_2}>R_2^S\right)}{\Pr\left(C^{DF,i}_{S,D_2}>R_2^S\right)}. \tag{30}$$

On the other hand, the $|\Phi|$ denotes the size of Φ and the ψ_2 in (28) can be given as

$$\psi_2=\binom{m}{k}\left[\Pr\left(C^{DF,i}_{S,D_2}<R_2^S\right)\right]^{m-k}\left[\Pr\left(C^{DF,i}_{S,D_2}>R_2^S\right)\right]^k. \tag{31}$$

Combining (26), (27), (28), (30) and (31), by applying some algebraic manipulations we can obtain the expression P^{DF}_{TRS,Θ_m} as

$$P^{DF}_{TRS,\Theta_m}=\left[1-\Pr\left(C^{DF,i}_{S,D_1}>R_1^S,C^{DF,i}_{S,D_2}>R_2^S\right)\right]^m. \tag{32}$$

Unfortunately, it is difficult to derive the closed-form expression of (32), but it can be evaluated by using numerical simulations. To further obtain a theoretical result, the upper bounds of received SINRs (2) and (6) are exploited in the closed-form expression derivation of (32). Therefore, the closed-form expression of (32) can be provided in the following lemma.

Lemma 2: The closed-form expression of SOP for the DF-based NOMA system on the condition $|\Theta|=m$ can be approximated as

$$P^{DF}_{TRS,\Theta_m}=\left[1-\left(1+d_e^{\alpha}\right)e^{-(1+d_1^{\alpha})\tau_1}\left(\frac{1}{\Delta}\left(1-e^{-\Delta\tau_2}\right)\times\left(1-\xi\right)+\frac{\xi e^{-c_n\tau_1}}{c_n\lambda_1+\Delta}\left(1-e^{-(c_n\lambda_1+\Delta)\tau_2}\right)\right)\right]^m, \tag{33}$$

where $\theta_j=2^{2R_j^S}$, $j\in(1,2)$, $\tau_1=\frac{\theta_1-1}{a_1\rho}$, $\tau_2=\frac{1+\frac{a_2}{a_1}-\theta_2}{a_2\rho_E\theta_2}$, $\lambda_1=\frac{\theta_1\rho_E}{\rho}$, $\Delta=\lambda_1\left(1+d_1^{\alpha}\right)+\left(1+d_e^{\alpha}\right)$ and $\xi=\frac{\pi}{2N}\sum_{n=1}^{N}\sqrt{1-\phi_n^2}\left(\phi_n+1\right)$. Note that (33) is derived on the condition of $a_1\theta_2<1$, otherwise $P^{DF}_{TRS,\Theta_m}=1$.

Proof: See Appendix B. ■

Combining **Lemma 1**, **Lemma 2** and (21) and applying some algebraic manipulations, the SOP of TRS scheme for the DF-based NOMA system can be provided in the following theorem.

Theorem 1: The closed-form expression of SOP for TRS scheme in the DF-based NOMA system is approximated as

$$P^{DF}_{TRS}=\left[1-\left(1-\xi\left(1-e^{-c_n\tau}\right)\right)\times\left(1+d_e^{\alpha}\right)e^{-(1+d_1^{\alpha})\tau_1}\times\left(\frac{1}{\Delta}\left(1-e^{-\Delta\tau_2}\right)\left(1-\xi\right)+\xi e^{-c_n\tau_1}\times\frac{1}{c_n\lambda_1+\Delta}\left(1-e^{-(c_n\lambda_1+\Delta)\tau_2}\right)\right)\right]^K. \tag{34}$$

B. OPTIMAL RELAY SELECTION

In this subsection ORS scheme is proposed, where the ORS is to minimize the SOP of the cooperative NOMA system. Based on above analysis, we can easily obtain the SOP of D_1 and D_2 with ith ($i\in\Theta$) relay as

$$P^{DF,i}_{out,D_1}=\Pr\left\{C^{DF,i}_{S,D_1}<R_1^S\right\}, \tag{35}$$

and

$$P^{DF,i}_{out,D_2}=\Pr\left\{C^{DF,i}_{S,D_2}<R_2^S\right\}, \tag{36}$$

respectively. As the ORS scheme proposed is to minimize the SOP of the DF/AF-based NOMA system, we further define

$$\chi_i=\min\left\{\frac{C^{DF,i}_{S,D_1}}{R_1^S},\frac{C^{DF,i}_{S,D_2}}{R_2^S}\right\}. \tag{37}$$

Hence, the RS criterion to optimal the secrecy performance (i.e., minimize the SOP of the NOMA system) is expressed as

$$i^*_{ORS}=\arg\max_{i\in\Theta}\left\{\chi_i\right\}. \tag{38}$$

On the condition of $|\Theta|=m$, the SOP of ORS scheme for the DF-based NOMA system can be given as

$$\begin{aligned}P^{DF}_{ORS,\Theta_m}&=\prod_{i=1}^{m}\Pr\left(\chi_i<1\right)\\&=\left(1-\Pr\left(\min\left\{\frac{C^{DF,i}_{S,D_1}}{R_1^S},\frac{C^{DF,i}_{S,D_2}}{R_2^S}\right\}>1\right)\right)^m\\&=\left(1-\Pr\left(C^{DF,i}_{S,D_1}>R_1^S,C^{DF,i}_{S,D_2}>R_2^S\right)\right)^m.\end{aligned} \tag{39}$$

Remark 1: It is obvious that the closed-form expression of P^{DF}_{ORS,Θ_m} is the same as the closed-form expression of P^{DF}_{TRS,Θ_m} in (33). Similarly, the closed-form expression of SOP for the DF-based NOMA ORS scheme P^{DF}_{ORS} is the same as the closed-form expression of P^{DF}_{TRS} in (34). According to the definition of the cooperative NOMA, D_2 should be quickly connected with a low data rate, while D_1 should be served opportunistically. Compared to D_1, D_2 is easy to obtain a secure communication, therefore the secrecy performance of TRS/ORS schemes for DF-based NOMA system is mainly determined by the D_1.

C. BENCHMARKS FOR TRS AND ORS SCHEMES

In this subsection, the RRS scheme was considered as a benchmark for comparison purposes, where the relay R_i is selected randomly, i.e., the selected R_i maybe not the optimal one for the NOMA RS schemes. In this case, the RRS scheme is capable of being regarded as the special case for TRS/ORS schemes with $K = 1$, which is independent of the number of relays. According to **Theorem 1** and **Remark 1**, for the TRS/ORS schemes, the SOP of RRS scheme for the DF-based NOMA system can be easily approximated as

$$\begin{aligned} P^{DF}_{RRS} = 1 &- \left(1 - \xi\left(1 - e^{-c_n\tau}\right)\right) \times \left(1 + d_e^{\alpha}\right) e^{-\left(1+d_1^{\alpha}\right)\tau_1} \\ &\times \left(\frac{1}{\Delta}\left(1 - e^{-\Delta\tau_2}\right)(1-\xi) + \xi e^{-c_n\tau_1}\right. \\ &\left.\times \frac{1}{c_n\lambda_1 + \Delta}\left(1 - e^{-(c_n\lambda_1+\Delta)\tau_2}\right)\right). \end{aligned} \tag{40}$$

D. SECRECY DIVERSITY ORDER ANALYSIS

In this section, to gain more insights for these RS schemes, the secrecy diversity order is obtained in high SNR region according to the above analysis results. The secrecy diversity order [27] can be defined as

$$d = -\lim_{\rho\to\infty} \frac{\log\left(P(\rho)\right)}{\log\rho}. \tag{41}$$

1) TWO-STAGE RELAY SELECTION

Based on (34), when $\rho \to \infty$, according to $e^{-x} \approx 1 - x$ ($x \to 0$), we can derive the asymptotic SOP of TRS scheme for the DF-based NOMA system in the following corollary.

Corollary 1: The asymptotic SOP of TRS scheme for the DF-based NOMA system at high SNR is given by

$$\begin{aligned} &P^{DF,\infty}_{TRS} \\ &\approx \left[1 - (1 - \xi c_n\tau)\left(1 + d_e^{\alpha}\right)\left(1 - \left(1 + d_1^{\alpha}\right)\tau_1\right)\right. \\ &\quad\times\left(\frac{(1-\xi)}{\left(1 + d_e^{\alpha}\right)}\left(1 - C_2\left(1 - \lambda_1 C_1\right)\right) + \frac{\xi\left(1 - c_n\tau_1\right)}{\left(1 + d_e^{\alpha}\right)}\right. \\ &\quad\left.\left.\times\left(1 - C_2\left(1 - \lambda_1\tau_2\left(1 + d_1^{\alpha} + c_n\right)\right)\right)\right)\right]^K, \end{aligned} \tag{42}$$

where $C_1 = \left(1 + d_1^{\alpha}\right)\tau_2$, $C_2 = e^{-\left(1+d_e^{\alpha}\right)\tau_2}$.

Substituting (42) into (41), we can obtain $d^{DF}_{TRS} = K$.

2) OPTIMAL RELAY SELECTION

Based on **Remark 1** and (42), we can obtain $d^{DF}_{ORS} = K$.

Remark 2: The secrecy diversity order of ORS scheme for the DF-based NOMA system is K, which is the same as the secrecy diversity order of TRS scheme.

3) RANDOM RELAY SELECTION

Based on the derivation (40) and (42), the asymptotic SOP of RRS scheme for the DF-based NOMA system at high SNR can be given as

$$\begin{aligned} &P^{DF,\infty}_{RRS} \\ &\approx 1 - (1 - \xi c_n\tau)\left(1 + d_e^{\alpha}\right)\left(1 - \left(1 + d_1^{\alpha}\right)\tau_1\right) \\ &\quad\times\left(\frac{(1-\xi)}{\left(1 + d_e^{\alpha}\right)}\left(1 - C_2\left(1 - \lambda_1 C_1\right)\right) + \frac{\xi\left(1 - c_n\tau_1\right)}{\left(1 + d_e^{\alpha}\right)}\right. \\ &\quad\left.\times\left(1 - C_2\left(1 - \lambda_1\tau_2\left(1 + d_1^{\alpha} + c_n\right)\right)\right)\right). \end{aligned} \tag{43}$$

Remark 3: Substituting (43) into (41), we can obtain that the secrecy diversity order of RRS scheme for the DF-based NOMA system is one.

IV. SECRECY PERFORMANCE EVALUATION FOR AF-BASED NOMA SYSTEM

In this section, the secrecy performance of the AF-based NOMA system is investigated with TRS and ORS schemes, respectively.

A. TWO-STAGE RELAY SELECTION SCHEME

For AF-based NOMA system, all the relays (K relays) can amplify and forward the superposed signal to the users. Therefore, different from (24) in DF-based NOMA system, the condition of relay selection in the first stage is $\Phi = \arg\limits_{i}\left\{C^{AF,i}_{S,D2} > R_2^S, 1 \le i \le K\right\}$. Refer to the analysis and derivation in the DF-based system (III, A), the SOP expression of TRS scheme for the AF-based NOMA system is given as

$$P^{AF}_{TRS} = \left[1 - \Pr\left(C^{AF,i}_{S,D_1} > R_1^S, C^{AF,i}_{S,D_2} > R_2^S\right)\right]^K. \tag{44}$$

Applying some algebraic manipulations, the SOP of TRS scheme for the AF-based NOMA system can be provided in the following theorem.

Theorem 2: The closed-form expression of SOP for TRS scheme in the AF-based NOMA system is approximated as

$$\begin{aligned} P^{AF}_{TRS} = &\left[1 - \left(1 + d_e^{\alpha}\right)e^{-\left(1+d_1^{\alpha}\right)\tau_1}\left(\frac{1}{\Delta}\left(1 - e^{-\Delta\tau_2}\right)(1-\xi)\right.\right. \\ &\left.\left.+ \xi e^{-c_n\tau_1}\frac{1}{c_n\lambda_1 + \Delta}\left(1 - e^{-(c_n\lambda_1+\Delta)\tau_2}\right)\right)\right]^K. \end{aligned} \tag{45}$$

Note that (45) is derived on the condition of $a_1\theta_2 < 1$, otherwise $P^{AF}_{TRS} = 1$.

Proof: See Appendix C. ■

B. OPTIMAL RELAY SELECTION SCHEME

Similar to TRS in AF-based NOMA system, referring the analysis and derivation in the DF-based system (III, B), the SOP expression of ORS scheme for the AF-based NOMA system is given as

$$P_{ORS}^{AF} = \left[1 - \Pr\left(C_{S,D_1}^{AF,i} > R_1^S, C_{S,D_2}^{AF,i} > R_2^S\right)\right]^K. \quad (46)$$

Remark 4: It is obvious that the closed-form expression of SOP for ORS scheme in the AF-based NOMA system P_{ORS}^{AF} is the same as the closed-form expression (45). As ***Remark 1****, the secrecy performance of TRS/ORS schemes for AF-based NOMA system is mainly determined by the D_1.*

Based on the analytical process of the SOP for TRS/ORS schemes in the DF/AF-based NOMA system, i.e., according to (33), (34) and (45), we can obtain the conclusion in the following Corollary.

Corollary 2: The SOP of TRS/ORS schemes for the DF-based NOMA system is always greater than that of AF-based NOMA system when not all DF relays successfully decode the received signals ($m < K$). The SOP of TRS/ORS schemes for the DF-based system is the same to that of AF-based NOMA system when all DF relays successfully decode the received signals ($m = K$).

C. BENCHMARKS FOR TRS AND ORS SCHEMES

Similarly, according to **Theorem 2.** and **Remark 4.**, for the TRS/ORS schemes, the SOP of RRS scheme for the AF-based NOMA system can be easily approximated as

$$P_{RRS}^{AF} = 1 - \left(1 + d_e^{\alpha}\right) e^{-\left(1+d_1^{\alpha}\right)\tau_1} \left(\frac{1}{\Delta}\left(1 - e^{-\Delta\tau_2}\right)(1-\xi) + \xi e^{-c_n\tau_1} \frac{1}{c_n\lambda_1 + \Delta}\left(1 - e^{-(c_n\lambda_1+\Delta)\tau_2}\right)\right). \quad (47)$$

D. SECRECY DIVERSITY ORDER ANALYSIS

1) TWO-STAGE RELAY SELECTION

Based on (45), when $\rho \to \infty$, according to $e^{-x} \approx 1 - x$ ($x \to 0$), we can derive the asymptotic SOP of TRS scheme for the AF-based NOMA system in the following corollary.

Corollary 3: The asymptotic SOP of TRS scheme for the AF-based NOMA system at high SNR is given by

$$P_{TRS}^{AF,\infty} \approx [1 - \left(1 + d_e^{\alpha}\right)\left(1 - \left(1 + d_1^{\alpha}\right)\tau_1\right)\left(\frac{(1-\xi)}{\left(1 + d_e^{\alpha}\right)} \times \left(1 - C_2\left(1 - \lambda_1 C_1\right)\right) + \frac{\xi\left(1 - c_n\tau_1\right)}{\left(1 + d_e^{\alpha}\right)} \times \left(1 - C_2\left(1 - \lambda_1\tau_2\left(1 + d_1^{\alpha} + c_n\right)\right)\right)\right)]^K. \quad (48)$$

Substituting (48) into (41), we can obtain $d_{TRS}^{AF} = K$.

2) OPTIMAL RELAY SELECTION

Based on **Remark 4** and (48), we can obtain $d_{ORS}^{AF} = K$.

TABLE 1. Secrecy diversity orders for DF/AF-based NOMA RS schemes.

Relaying protocol	RS scheme	D
DF	TRS	K
	ORS	K
	RRS	1
AF	TRS	K
	ORS	K
	RRS	1

Remark 5: The secrecy diversity order of ORS scheme for the AF-based NOMA system is K, which is the same as the secrecy diversity order of TRS scheme.

3) RANDOM RELAY SELECTION

Based on the derivation (47) and (48), the asymptotic SOP of RRS scheme for the AF-based NOMA system at high SNR can be given as

$$P_{RRS}^{AF,\infty} \approx 1 - \left(1 + d_e^{\alpha}\right)\left(1 - \left(1 + d_1^{\alpha}\right)\tau_1\right)\left(\frac{(1-\xi)}{\left(1 + d_e^{\alpha}\right)} \times \left(1 - C_2\left(1 - \lambda_1 C_1\right)\right) + \frac{\xi\left(1 - c_n\tau_1\right)}{\left(1 + d_e^{\alpha}\right)} \times \left(1 - C_2\left(1 - \lambda_1\tau_2\left(1 + d_1^{\alpha} + c_n\right)\right)\right)\right). \quad (49)$$

Remark 6: Substituting (49) into (41), we can obtain that the secrecy diversity order of RRS scheme for the AF-based NOMA system is one.

To get intuitional insights, as shown in TABLE I, the secrecy diversity orders of RS schemes for the DF/AF-based NOMA systems are summarized to illustrate the comparison between them, where D denotes the secrecy diversity order.

TABLE 2. Table of parameters for simulation results.

Monte Carlo simulations repeated	10^6 iterations
Power allocation coefficients of NOMA	$a_1 = 0.2, a_2 = 0.8$
Targeted secrecy data rates	$R_1^S = 1, R_2^S = 0.1$ BPCU
Targeted data rates	$R_1^{th} = 2, R_2^{th} = 0.2$ BPCU
Path loss exponent	$\alpha = 2$
The radius of a disc region	$R_D = 2$ m
Average SNR of illegal link	$\rho_E = 10$ dB
The distance between the BS and D_1	10 m
The distance between the BS and D_2	12 m
The distance between the BS and Eve	100 m

V. NUMERICAL RESULTS

In this section, simulation results are provided to evaluate the secrecy outage performance of the TRS and ORS schemes for DF/AF-based NOMA systems. The simulation parameters used in this section are presented in Table II [27], where BPCU is an abbreviation for bit per channel use. The complexity-vs-accuracy tradeoff parameter is $N = 20$. Additionally, α is the path loss exponent usually satisfying $2 \le \alpha \le 6$. In this section, the pass loss exponent is selected as $\alpha = 2$ [27], [29]. To ensure the validity of numerical

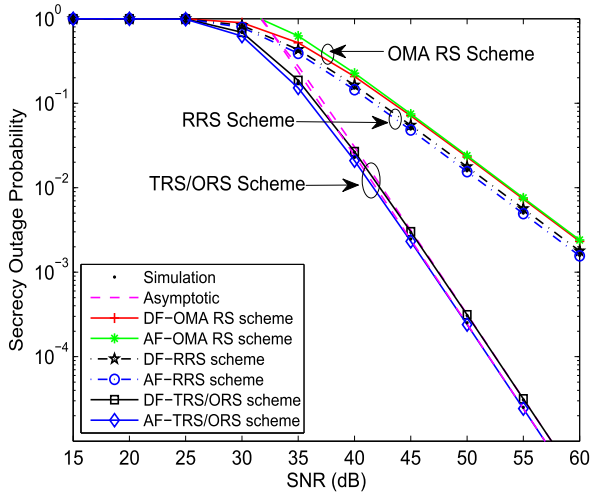

FIGURE 2. The SOP versus transmit SNR for TRS/ORS schemes with $K = 2$; $R_1^S = 1$ BPCU, $R_2^S = 0.1$ BPCU and $R_1^{th} = 2$ BPCU, $R_2^{th} = 0.2$ BPCU.

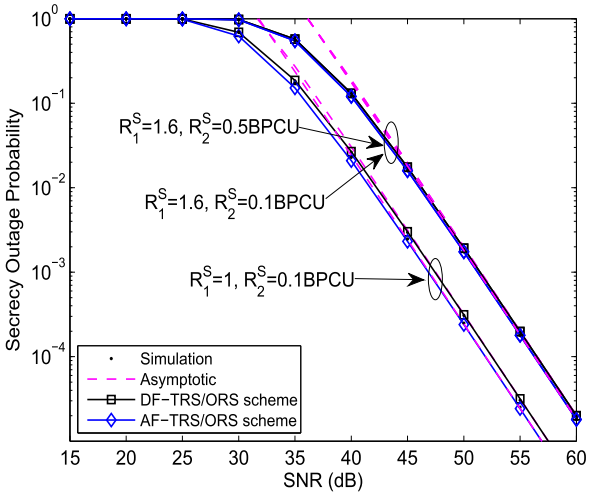

FIGURE 3. The SOP versus transmit SNR for TRS/ORS schemes with different targeted secrecy data rates; $K = 2$ and $R_1^{th} = 2$ BPCU, $R_2^{th} = 0.2$ BPCU.

results, the numerical results of the SOP with different path loss exponent are also presented in the following. Except RRS scheme of DF/AF-based NOMA systems, the performance of OMA-based RS scheme is also considered as a benchmark for comparison, where the total communication process is finished in four slots. The BS sends information x_1 and x_2 to relay R_i in the first and second slot, respectively. In the third and fourth slot, R_i forwards the information x_1 and x_2 to D_1 and D_2, respectively.

Fig. 2 plots the SOP of TRS/ORS schemes versus transmit SNR with $K = 2$. The black and blue solid curves are the SOP of TRS/ORS schemes for DF and AF NOMA, corresponding to the approximate results derived in (34) and (45), respectively. The black and blue dash dotted curves represent the approximate SOP of RRS scheme for DF and AF NOMA derived in (40) and (47), respectively. It is obvious that the SOP curves match precisely with the Monte Carlo simulations results. Moreover, the secrecy outage performance of the TRS/ORS schemes outperforms the RRS scheme. The asymptotic SOP curves of the TRS/ORS schemes for DF/AF-based NOMA systems are plotted according to the derivation in (42) and (48), respectively. As can be observed that the asymptotic curves well approximate the analytical performance curves in the high SNR region. A specific observation is that the secrecy diversity orders of RRS scheme for DF/AF-based NOMA systems are one, which is also confirmed by the insights in **Remark 3** and **Remark 6**. Another observation is that NOMA TRS/ORS schemes are superior to OMA-based RS scheme. This is due to the fact that NOMA RS schemes are able to enhance the spectral efficiency compared to OMA. We also observed that the secrecy outage performance of these RS schemes for AF-based NOMA is better than that of DF-based NOMA. The reason is that not all DF relays successfully decode the received signals, especially when the target rate is high, which verifies the conclusion in **Corollary 2**. Compared with the secrecy outage behaviors of [40], where the sop of the NOMA systems tend to be constants when SNR is larger enough. An important observation is that the SOP of TRS/ORS schemes become smaller and the gains become more evident in the high SNR region.

Fig. 3 plots the SOP of TRS/ORS schemes versus transmit SNR with different targeted secrecy data rates. One can observe that with increasing of R_1^S, the SOP of TRS/ORS for AF/DF-based NOMA systems becomes worse. This is because increasing R_1^S will lead to the threshold of decoding higher, which reduces the secrecy performance of D_1. It is shown that the secrecy outage behaviors of the TRS/ORS scheme are hardly affected by the increasing of R_2^S. This phenomenon can be explained as that D_2 should be quickly connected with a low data rate, while D_1 should be served opportunistically according to the definition of the cooperative NOMA. D_2 is easy to obtain a secure communication compared to D_1, therefore the secrecy performance of the system becomes worse when the secrecy performance of D_1 deteriorates. It is worth noting that the setting of reasonable target secrecy rates for NOMA users is prerequisite in different scenarios.

Fig. 4 plots the SOP of TRS/ORS schemes versus transmit SNR with different targeted data rates. The black and blue curves denote the SOP of TRS/ORS schemes based on DF and AF protocols, respectively. The figure shows that the secrecy outage behaviors of the AF-based TRS/ORS schemes are not affected by adjusting of R_1^{th} and R_2^{th}. Similar to Fig. 3, with increasing of R_1^{th}, the SOP of TRS/ORS schemes for the DF-based sytem gets worse, while it is hardly affected by adjusting of R_2^{th}. This is due to the fact that the targeted data rate affects the outage probability of decoding at DF relay, at the same time D_2 with a lower targeted data rate is easier to decode successfully at the DF relay than D_1. Furthermore, the SOP of TRS/ORS schemes for DF/AF-based NOMA systems tends to coincide, when the targeted data rates become smaller. This verifies the conclusion in

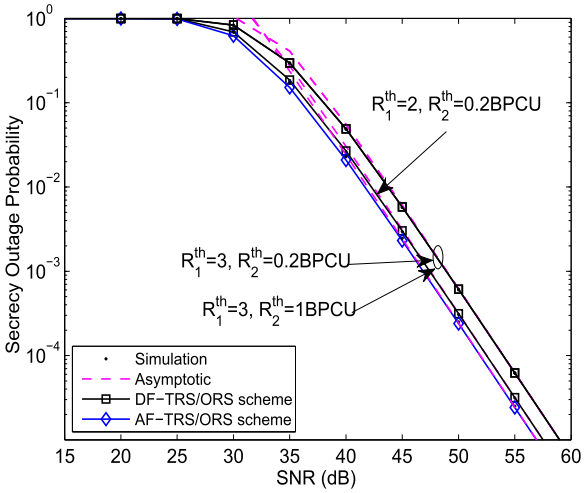

FIGURE 4. The SOP versus transmit SNR for TRS/ORS schemes with different targeted data rates; $K = 2$ and $R_1^S = 1$ BPCU, $R_2^S = 0.1$ BPCU.

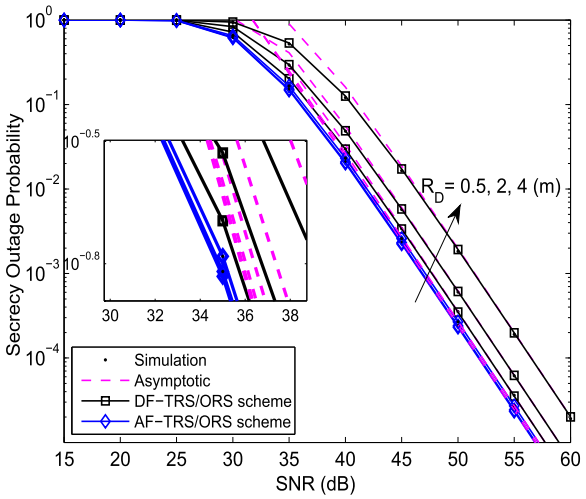

FIGURE 5. The SOP versus transmit SNR for TRS/ORS schemes with different R_D, $K = 2$; $R_1^S = 1$ BPCU, $R_2^S = 0.1$ BPCU and $R_1^{th} = 3$ BPCU, $R_2^{th} = 0.2$ BPCU.

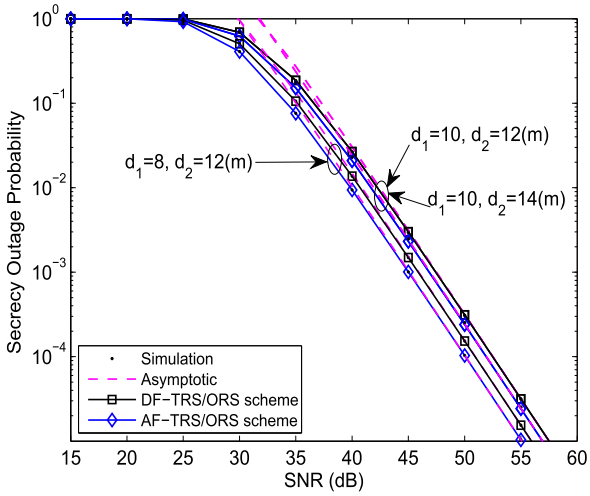

FIGURE 6. The SOP versus transmit SNR for TRS/ORS schemes with different d_1 and d_2, $K = 2$; $R_1^S = 1$ BPCU, $R_2^S = 0.1$ BPCU and $R_1^{th} = 2$ BPCU, $R_2^{th} = 0.2$ BPCU.

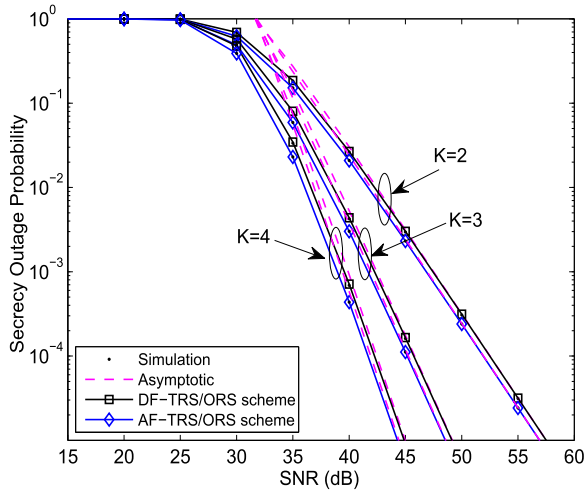

FIGURE 7. The SOP versus transmit SNR for TRS/ORS schemes with $K = 2, 3, 4$; $R_1^S = 1$ BPCU, $R_2^S = 0.1$ BPCU and $R_1^{th} = 2$ BPCU, $R_2^{th} = 0.2$ BPCU.

Corollary 2 that the SOP of TRS/ORS schemes for DF/AF-based NOMA system will be the same when all the DF relays can successfully decode the received signals.

Fig. 5 plots the SOP of TRS/ORS schemes versus transmit SNR with different radius R_D. It is observed that the security performance of the system with TRS/ORS scheme deteriorates with increasing radius. The impact is significant on the secrecy behavior of DF-based NOMA system. Since the path loss will increase as the relay distribution radius increases, which especially affects the outage probability of decoding at DF relay. However, the blue curves tend to coincide, which means that the secrecy behaviors of the AF-based system is slightly affected with adjustment of R_D. This is mainly due to the characteristics of AF relay, i.e., decoding outage events cannot occur at AF relay. Fig. 6 plots the SOP of TRS/ORS schemes versus SNR with different d_1 and d_2. Similar to Fig. 5, we can observe that the secrecy performance of the system deteriorates with increasing d_1. However, the secrecy performance of the system is independent of the adjustment of d_2, as shown in the closed-form expression of SOP (34) and (45), i.e., the secrecy performance of the system is not affected by the channel between relays and D_2. This is because that the instantaneous SINRs at D_2 tends to $\frac{a_2}{a_1}$ in high SNR, which are exploited in the derivation of (34) and (45).

Fig. 7 plots the SOP of TRS/ORS schemes versus transmit SNR with $K = 2, 3, 4$. As can be seen that the analytical curves perfectly match with the simulation results, while the approximations match the analytical performance curves in the high SNR region. It is shown that the number of relays in the networks considered strongly affect the secrecy performance of TRS/ORS schemes for the DF/AF-based NOMA systems. With the number of relays increases, the secrecy behaviors of the DF/AF-based systems become better. This is because more relays bring higher diversity gains, which

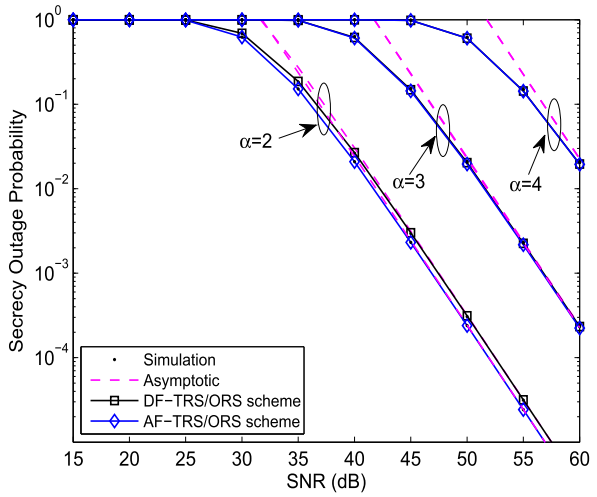

FIGURE 8. The SOP versus transmit SNR for TRS/ORS schemes with different pass loss exponent α, $K = 2$; $R_1^S = 1$ BPCU, $R_2^S = 0.1$ BPCU and $R_1^{th} = 2$ BPCU, $R_2^{th} = 0.2$ BPCU.

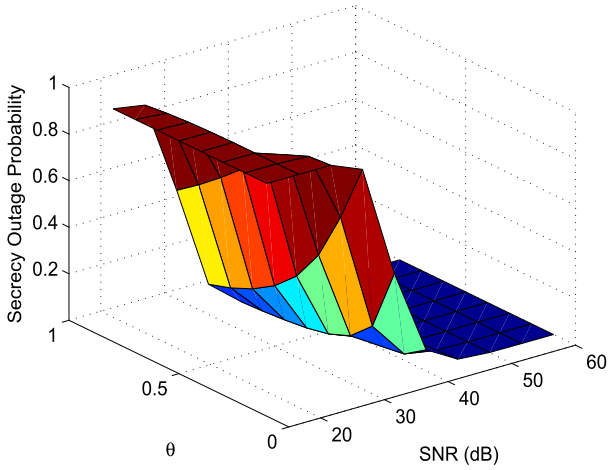

FIGURE 9. The SOP of DF-based NOMA system versus transmit SNR and θ for TRS/ORS schemes with $K = 2$; $R_1^S = 1$ BPCU, $R_2^S = 0.1$ BPCU and $R_1^{th} = 2$ BPCU, $R_2^{th} = 0.2$ BPCU.

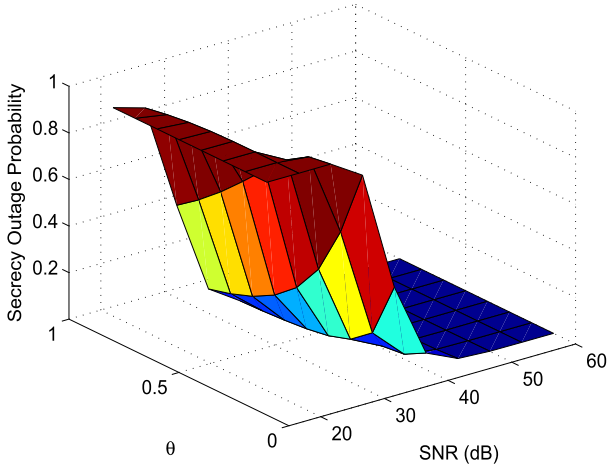

FIGURE 10. The SOP of AF-based NOMA system versus transmit SNR and θ for TRS/ORS schemes with $K = 2$; $R_1^S = 1$ BPCU, $R_2^S = 0.1$ BPCU and $R_1^{th} = 2$ BPCU, $R_2^{th} = 0.2$ BPCU.

improves the reliability of the cooperative networks [27]. Another observation is that the NOMA TRS/ORS schemes provide a diversity order that is equal to the number of the relays (K), which verifies the conclusions in **Corollary 1**, **Remark 2**, **Corollary 3** and **Remark 5**. As it is observed, more secrecy diversity gains can be achieved with the proposed TRS/ORS schemes compared to the NOMA system with only one relay [40].

As a further development, Fig. 8 plots the SOP of TRS/ORS schemes versus transmit SNR with different path loss exponent. It obviously that the performance of TRS/ORS schemes for the DF/AF-based NOMA systems is strongly affected by the path loss exponent considered in the networks. With the path loss exponent increasing, the performance of the NOMA system deteriorates. It can be observed that the curves with different path loss exponent have the same slopes, as the secrecy diversity orders provided by TRS/ORS schemes are only related to the number of relays, i.e., the secrecy diversity orders are equal to the number of the relays (K), which verifies the conclusions in **Corollary 1**, **Remark 2**, **Corollary 3** and **Remark 5** again.

In order to illustrate the impact of dynamic power allocation factor on the NOMA secrecy performance, Fig. 9 and Fig. 10 plot the SOP of TRS/ORS schemes for DF/AF-based NOMA systems versus transmit SNR and θ, respectively; in which $\theta \in [0, 1]$ denotes the dynamic power allocation factor. Especially, when a_1 is set to be $a_1 = \theta$, $a_2 = 1 - \theta$. The analytical results of the DF/AF-based NOMA systems are calculated from (34) and (45). These figures show that the secrecy performance of the NOMA system becomes better as transmit SNR increases, which is the same as the traditional trend, where the SOP always decreases as the transmit SNR increases. We also can observe that the optimal SOP with different values is affected by the dynamic power allocation factor. It is critical to select beneficial system parameters. Furthermore, optimizing the power allocation factor is capable of further improving the system secrecy performance, which motivates us to investigate optimal power allocation algorithms in our future work.

VI. CONCLUSION

This paper has investigated TRS/ORS schemes for the DF/AF-based NOMA systems insightfully. Spatial locations of relays have been modeled by invoking stochastic geometry. New closed-form expressions of SOP of TRS/ORS schemes have been derived for DF/AF-based NOMA systems. Based on the analytical results, the DF/AF-based NOMA systems with TRS/ORS schemes are capable of providing the secrecy diversity order of K, which is equal to the number of relays. Simulation results have verified that the DF/AF-based NOMA systems with TRS/ORS schemes achieved better secrecy outage behaviors than RRS and OMA-based RS schemes. It was shown that TRS/ORS schemes for the DF/AF-based systems achieved lower SOP with increasing the number of relays. The secrecy outage behaviors of the

AF-based NOMA system was superior to that of DF-based NOMA system. Furthermore, the secrecy behaviors of the DF/AF-based NOMA systems were impacted by the power allocation between NOMA users. It is significant to further enhance the system secrecy performance by optimizing the power allocation factor.

APPENDIX A

Combining (2), (3) and (22) and applying some algebraic manipulations, the Q in (22) can be rewritten as

$$\begin{aligned} Q = &\Pr\left(\left|h_{R_i}\right|^2 > \frac{2^{2R_1^{th}}-1}{a_1\rho},\right. \\ &\left.\left|h_{R_i}\right|^2 > \frac{2^{2R_2^{th}}-1}{\left(a_2-\left(a_1 2^{2R_2^{th}}-1\right)\right)\rho}\right) \\ = &\Pr\left(\left|h_{R_i}\right|^2 > \tau\right), \end{aligned} \tag{A.1}$$

where $\tau = \max\left(\frac{2^{2R_1^{th}}-1}{a_1\rho}, \frac{2^{2R_2^{th}}-1}{\left(a_2-\left(a_1 2^{2R_2^{th}}-1\right)\right)\rho}\right)$.

According to $h_{R_i} = \frac{h_{SR_i}}{\sqrt{1+d_{SR_i}^{\alpha}}}$, we have $\left|h_{R_i}\right|^2 = \frac{\left|h_{SR_i}\right|^2}{1+d_{SR_i}^{\alpha}}$. As [14] the CDF $F_{|h_{R_i}|^2}$ of $\left|h_{R_i}\right|^2$ is given by

$$F_{|h_{R_i}|^2}(x) = \frac{2}{R_D^2}\int_0^{R_D}\left(1-e^{-(1+r^{\alpha})x}\right)rdr. \tag{A.2}$$

It is difficult to get the closed-form solution of (A.2), especially for some communication scenarios $\alpha > 2$. In this case, by using Gaussian-Chebyshev quadrature [42], the approximate expression of (A.2) for an arbitrary α can be given as

$$F_{|h_{R_i}|^2}(x) \approx \frac{\pi}{2N}\sum_{n=1}^{N}\sqrt{1-\phi_n^2}\left(1-e^{-c_n x}\right)(\phi_n+1). \tag{A.3}$$

By the virtue of approximate expression of CDF for $\left|h_{R_i}\right|^2$ in (A.3), Q in (A.1) can be further calculated as

$$Q = 1-\frac{\pi}{2N}\sum_{n=1}^{N}\sqrt{1-\phi_n^2}\left(1-e^{-c_n\tau}\right)(\phi_n+1). \tag{A.4}$$

Finally, substituting (A.4) into (22), (23) can be obtained. The proof is completed.

APPENDIX B

In (32), we assume $J_1 = \Pr\left(C_{S,D_1}^{DF,i} > R_1^S, C_{S,D_2}^{DF,i} > R_2^S\right)$. Based on the above analysis, J_1 can be further written as

$$\begin{aligned} J_1 = \Pr\Bigg(&\min\left\{\frac{1+\rho\left|h_{R_i}\right|^2 a_1}{1+\rho_E|h_e|^2 a_1}, \frac{1+\rho|h_1|^2 a_1}{1+\rho_E|h_e|^2 a_1}\right\} > \theta_1, \\ &\min\left\{\frac{1+\frac{\rho|h_{R_i}|^2 a_2}{\rho|h_{R_i}|^2 a_1+1}}{1+\rho_E|h_e|^2 a_2}, \frac{1+\frac{\rho|h_2|^2 a_2}{\rho|h_2|^2 a_1+1}}{1+\rho_E|h_e|^2 a_2}\right\} > \theta_2\Bigg), \end{aligned} \tag{B.1}$$

where $\theta_j = 2^{2R_j^S}, j \in (1,2)$. The closed-form expression of J_1 cannot be derived successfully. To further obtain a theoretical result of the SOP for TRS scheme in the DF-based NOMA system, the upper bounds of the SINRs $\frac{\rho|h_{R_i}|^2 a_2}{\rho|h_{R_i}|^2 a_1+1}$ and $\frac{\rho|h_2|^2 a_2}{\rho|h_2|^2 a_1+1}$ are $\frac{a_2}{a_1}$, which is exploited in the derivation of J_1, hence J_1 can be approximated as

$$\begin{aligned} J_1 \approx &\Pr\left(\min\left\{\frac{1+\rho\left|h_{R_i}\right|^2 a_1}{1+\rho_E|h_e|^2 a_1}, \frac{1+\rho|h_1|^2 a_1}{1+\rho_E|h_e|^2 a_1}\right\} > \theta_1,\right. \\ &\left.\min\left\{\frac{1+\frac{a_2}{a_1}}{1+\rho_E|h_e|^2 a_2}, \frac{1+\frac{a_2}{a_1}}{1+\rho_E|h_e|^2 a_2}\right\} > \theta_2\right) \\ = &\Pr\left(\min\left\{\left|h_{R_i}\right|^2, |h_1|^2\right\} > \lambda_1|h_e|^2+\tau_1, |h_e|^2 < \tau_2\right) \\ = &\int_0^{\tau_2}\left(1-F_{|h_{R_i}|^2}(\lambda_1 x+\tau_1)\right) \\ &\times\left(1-F_{|h_1|^2}(\lambda_1 x+\tau_1)\right)f_{|h_e|^2}(x)\,dx. \end{aligned} \tag{B.2}$$

where $\tau_1 = \frac{\theta_1-1}{a_1\rho}$, $\tau_2 = \frac{1+\frac{a_2}{a_1}-\theta_2}{a_2\rho_E\theta_2}$ with $a_1\theta_2 < 1$ and $\lambda_1 = \frac{\theta_1\rho_E}{\rho}$.

Define $d_{R_iD_j} \triangleq \sqrt{d_{SR_i}^2+d_j^2-2d_j d_{SR_i}\cos(\vartheta_i)}$ and $d_{R_iD_j} \gg d_{SR_i}$; To further simplify computational complexity, we also assume that the distance between R_i and D_j can be approximated as the distance between the BS and D_j, i.e., $d_{R_iD_j} \approx d_j$. Note that the distance d_j between the BS and D_j is a fixed value by this approximation. Hence we can obtain the corresponding approximate CDF of $\left|h_j\right|^2$ as

$$F_{|h_j|^2}(x) = 1-e^{-\left(1+d_j^{\alpha}\right)x}. \tag{B.3}$$

Similarly, we can obtain the corresponding approximate PDF of $|h_e|^2$ as

$$f_{|h_e|^2}(x) = \left(1+d_e^{\alpha}\right)e^{-(1+d_e^{\alpha})x}. \tag{B.4}$$

With the aid of (A.3), (B.3) and (B.4), J_1 can be calculated as

$$\begin{aligned} J_1 = &\int_0^{\tau_2}\left(1-\xi\left(1-e^{-c_n(\lambda_1 x+\tau_1)}\right)\right) \\ &\times\left(e^{-(1+d_1^{\alpha})(\lambda_1 x+\tau_1)}\right)\left(1+d_e^{\alpha}\right)e^{-(1+d_e^{\alpha})x}dx \\ = &\left(1+d_e^{\alpha}\right)e^{-(1+d_1^{\alpha})\tau_1}(1-\xi)\int_0^{\tau_2}e^{-\lambda_1(1+d_1^{\alpha})x-(1+d_e^{\alpha})x}dx \\ &+\left(1+d_e^{\alpha}\right)e^{-(1+d_1^{\alpha})\tau_1}\int_0^{\tau_2}\xi e^{-c_n(\lambda_1 x+\tau_1)} \\ &\times e^{-\lambda_1(1+d_1^{\alpha})x}e^{-(1+d_e^{\alpha})x}dx \\ = &\left(1+d_e^{\alpha}\right)e^{-(1+d_1^{\alpha})\tau_1}\left[\frac{1}{\Delta}\left(1-e^{-\Delta\tau_2}\right)(1-\xi)\right. \\ &\left.+\xi e^{-c_n\tau_1}\frac{1}{c_n\lambda_1+\Delta}\left(1-e^{-(c_n\lambda_1+\Delta)\tau_2}\right)\right], \end{aligned} \tag{B.5}$$

where $\Delta = \lambda_1\left(1+d_1^{\alpha}\right)+\left(1+d_e^{\alpha}\right)$ and $\xi = \frac{\pi}{2N}\sum_{n=1}^{N}\sqrt{1-\phi_n^2}(\phi_n+1)$. Note that (B.5) is derived on the

condition of $a_1\theta_2 < 1$. Substituting (B.5) into (32), we can obtain (33). The proof is completed.

APPENDIX C

In (44), we assume $J_2 = \Pr\left(C_{S,D_1}^{AF,i} > R_1^S, C_{S,D_2}^{AF,i} > R_2^S\right)$. It is difficult to obtain the closed form expression of J_2. Hence, exploiting the upper bound of received SINRs, $\gamma_{D_1}^{AF,i}$, $\gamma_{D_1\to E}^{AF,i}$, $\gamma_{D_2}^{AF,i} = \frac{a_2}{a_1}$ and $\gamma_{D_2\to E}^{AF,i}$ can be approximated as $\gamma_{D_1}^{AF,i} \approx \frac{|h_{R_i}|^2|h_1|^2 a_1\rho}{|h_1|^2+|h_{R_i}|^2}$, $\gamma_{D_1\to E}^{AF,i} \approx \frac{|h_{R_i}|^2|h_e|^2 a_1\rho\rho_E}{\rho_E|h_e|^2+\rho|h_{R_i}|^2}$, $\gamma_{D_2}^{AF,i} = \frac{a_2}{a_1}$ and $\gamma_{D_2\to E}^{AF,i} = \frac{|h_{R_i}|^2|h_e|^2 a_2\rho\rho_E}{\rho_E|h_e|^2+\rho|h_{R_i}|^2}$, respectively. J_2 can be approximated as

$$J_2 \approx \Pr\left(\frac{|h_{R_i}|^2|h_1|^2}{|h_1|^2+|h_{R_i}|^2} > \frac{\theta_1|h_{R_i}|^2|h_e|^2\rho\rho_E}{\rho\rho_E|h_e|^2+\rho|h_{R_i}|^2}+\tau_1, \frac{|h_{R_i}|^2|h_e|^2\rho\rho_E}{\rho_E|h_e|^2+\rho|h_{R_i}|^2} < \tau_1^*\right), \quad \text{(C.1)}$$

where $\tau_1^* = \frac{1+\frac{a_2}{a_1}-\theta_2}{a_2\theta_2}$, and (C.1) is established on the condition of $a_1 < \frac{1}{\theta_2}$.

By using the broad using inequality $\frac{xy}{(x+y)} \le \min\{x,y\}$, J_2 can be further approximated as

$$J_2 = \Pr\left(\min\left\{|h_1|^2, |h_{R_i}|^2\right\} > \min\left\{\lambda_1|h_e|^2, \theta_1|h_{R_i}|^2\right\}+\tau_1, \min\left\{\rho_E|h_e|^2, \rho|h_{R_i}|^2\right\} < \tau_1^*\right). \quad \text{(C.2)}$$

It is difficult to obtain a closed-form expression for (C.2). Therefore we denote

$$A = \min\left\{|h_1|^2, |h_{R_i}|^2\right\} > \min\left\{\lambda_1|h_e|^2, \theta_1|h_{R_i}|^2\right\} + \tau_1, \quad \text{(C.3)}$$

and

$$B = \min\left\{\rho_E|h_e|^2, \rho|h_{R_i}|^2\right\} < \tau_1^*, \quad \text{(C.4)}$$

respectively. According to the fact $P(A,B) = P(A) - P(A,\overline{B})$, where $\overline{B}$ presents complementary event of B. J_2 can be rewritten as

$$J_2 = J_3 - J_4, \quad \text{(C.5)}$$

where

$$J_3 = \Pr\left(\min\left\{|h_1|^2, |h_{R_i}|^2\right\} > \min\left\{\lambda_1|h_e|^2, \theta_1|h_{R_i}|^2\right\} + \tau_1\right), \quad \text{(C.6)}$$

and

$$J_4 = \Pr\left(\min\left\{|h_1|^2, |h_{R_i}|^2\right\} > \min\left\{\lambda_1|h_e|^2, \theta_1|h_{R_i}|^2\right\} + \tau_1, \min\left\{\rho_E|h_e|^2, \rho|h_{R_i}|^2\right\} > \tau_1^*\right), \quad \text{(C.7)}$$

respectively.

From above, we can observe that the event $A = \min\left\{|h_1|^2, |h_{R_i}|^2\right\} > \min\left\{\lambda_1|h_e|^2, \theta_1|h_{R_i}|^2\right\} + \tau_1$ can be written as $A = \min\left\{|h_1|^2, |h_{R_i}|^2\right\} > \lambda_1|h_e|^2 + \tau_1$, as the fact that $|h_{R_i}|^2 < \theta|h_{R_i}|^2 + \tau$. Then, J_3 can be rewritten as

$$\begin{aligned} J_3 &= \Pr\left(|h_1|^2 > \lambda_1|h_e|^2+\tau_1, |h_{R_i}|^2 > \lambda_1|h_e|^2+\tau_1\right) \\ &= \int_0^\infty \left(1 - F_{|h_{R_i}|^2}(\lambda_1 x+\tau_1)\right) \\ &\quad \times \left(1 - F_{|h_1|^2}(\lambda_1 x+\tau_1)\right) f_{|h_e|^2}(x)\,dx. \end{aligned} \quad \text{(C.8)}$$

In addition, J_4 can be rewritten as

$$\begin{aligned} J_4 &= \Pr\left(|h_1|^2 > \lambda_1|h_e|^2+\tau_1, |h_{R_i}|^2 > \lambda_1|h_e|^2+\tau_1, \rho_E|h_e|^2 > \tau_1^*, \rho|h_{R_i}|^2 > \tau_1^*\right) \\ &= \Pr\left(|h_1|^2 > \lambda_1|h_e|^2+\tau_1, |h_{R_i}|^2 > \lambda_1|h_e|^2+\tau_1, |h_e|^2 > \frac{\tau_1^*}{\rho_E} \triangleq \tau_2\right) \\ &= \int_{\tau_2}^\infty \left(1 - F_{|h_{R_i}|^2}(\lambda_1 x+\tau_1)\right) \\ &\quad \times \left(1 - F_{|h_1|^2}(\lambda_1 x+\tau_1)\right) f_{|h_e|^2}(x)\,dx. \end{aligned} \quad \text{(C.9)}$$

Combining (C.8), (C.9) and (C.5), we can obtain

$$\begin{aligned} J_2 &= \int_0^{\tau_2} \left(1 - F_{|h_{R_i}|^2}(\lambda_1 x+\tau_1)\right) \\ &\quad \times \left(1 - F_{|h_1|^2}(\lambda_1 x+\tau_1)\right) f_{|h_e|^2}(x)\,dx \\ &= \left(1+d_e^\alpha\right) e^{-(1+d_1^\alpha)\tau_1}\left[\frac{1}{\Delta}\left(1-e^{-\Delta\tau_2}\right)(1-\xi)\right. \\ &\quad \left.+\xi e^{-c_n\tau_1}\frac{1}{c_n\lambda_1+\Delta}\left(1-e^{-(c_n\lambda_1+\Delta)\tau_2}\right)\right]. \end{aligned} \quad \text{(C.10)}$$

Note that (C.9) and (C.10) are derived on the condition of $a_1\theta_2 < 1$. Substituting (C.10) into (44), we can obtain (45). The proof is completed.

REFERENCES

[1] S. M. R. Islam, N. Avazov, O. A. Dobre, and K.-S. Kwak, "Power-domain non-orthogonal multiple access (NOMA) in 5G systems: Potentials and challenges," *IEEE Commun. Surveys Tuts.*, vol. 19, no. 2, pp. 721–742, 2nd Quart., 2017.
[2] Z. Ding, Y. Liu, J. Choi, Q. Sun, M. Elkashlan, C.-L. I, and H. V. Poor, "Application of non-orthogonal multiple access in LTE and 5G networks," *IEEE Commun. Mag.*, vol. 55, no. 2, pp. 185–191, Feb. 2017.
[3] D. Tse and P. Viswanath, *Fundamentals of Wireless Communication*. Cambridge, U.K.: Cambridge Univ. Press, 2005.
[4] T. M. Cover and J. A. Thomas, *Elements of Information Theory*, 6th ed. New York, NY, USA: Wiley, 1991.
[5] S. Verdu and S. Verd, *Multiuser Detection*, Cambridge, U.K.: Cambridge Univ. Press, 1998.
[6] Z. Ding, Z. Yang, P. Fan, and H. V. Poor, "On the performance of non-orthogonal multiple access in 5G systems with randomly deployed users," *IEEE Signal Process. Lett.*, vol. 21, no. 12, pp. 1501–1505, Dec. 2014.
[7] Y. Liu, Z. Qin, M. Elkashlan, Z. Ding, A. Nallanathan, and L. Hanzo, "Nonorthogonal multiple access for 5G and beyond," *Proc. IEEE*, vol. 105, no. 12, pp. 2347–2381, Dec. 2017.
[8] X. Yue, Z. Qin, Y. Liu, S. Kang, and Y. Chen, "A unified framework for non-orthogonal multiple access," *IEEE Trans. Commun.*, vol. 66, no. 11, pp. 5346–5359, Nov. 2018.
[9] S. Timotheou and I. Krikidis, "Fairness for non-orthogonal multiple access in 5G systems," *IEEE Signal Process. Lett.*, vol. 22, no. 10, pp. 1647–1651, Oct. 2015.

[10] F. Liu and M. Petrova, "Performance of proportional fair scheduling for downlink PD-NOMA networks," *IEEE Trans. Wireless Commun.*, vol. 17, no. 10, pp. 7027–7039, Oct. 2018.
[11] Z. Ding, M. Peng, and H. V. Poor, "Cooperative non-orthogonal multiple access in 5G systems," *IEEE Commun. Lett.*, vol. 19, no. 8, pp. 1462–1465, Aug. 2015.
[12] Z. Zhang, Z. Ma, M. Xiao, Z. Ding, and P. Fan, "Full-duplex device-to-device-aided cooperative nonorthogonal multiple access," *IEEE Trans. Veh. Technol.*, vol. 66, no. 5, pp. 4467–4471, May 2017.
[13] X. Yue, Y. Liu, S. Kang, A. Nallanathan, and Z. Ding, "Exploiting full/half-duplex user relaying in NOMA systems," *IEEE Trans. Commun.*, vol. 66, no. 2, pp. 560–575, Feb. 2018.
[14] Y. Liu, Z. Ding, M. Elkashlan, and H. V. Poor, "Cooperative non-orthogonal multiple access with simultaneous wireless information and power transfer," *IEEE J. Sel. Areas Commun.*, vol. 34, no. 4, pp. 938–953, Apr. 2016.
[15] Z. Wang, X. Yue, and Z. Peng, "Full-duplex user relaying for NOMA system with self-energy recycling," *IEEE Access*, vol. 6, pp. 67057–67069, 2018.
[16] X. Liang, Y. Wu, D. W. K. Ng, Y. Zuo, S. Jin, and H. Zhu, "Outage performance for cooperative NOMA transmission with an AF relay," *IEEE Commun. Lett.*, vol. 21, no. 11, pp. 2428–2431, Nov. 2017.
[17] J. Men, J. Ge, and C. Zhang, "Performance analysis of non-orthogonal multiple access for relaying networks over Nakagami-*m* fading channels," *IEEE Trans. Veh. Technol.*, vol. 66, no. 2, pp. 1200–1208, Feb. 2017.
[18] X. Yue, Y. Liu, S. Kang, and A. Nallanathan, "Performance analysis of NOMA with fixed gain relaying over Nakagami-*m* fading channels," *IEEE Access*, vol. 5, pp. 5445–5454, 2017.
[19] T. M. C. Chu and H.-J. Zepernick, "Performance of a non-orthogonal multiple access system with full-duplex relaying," *IEEE Commun. Lett.*, vol. 22, no. 10, pp. 2084–2087, Oct. 2018.
[20] D. Wan, M. Wen, F. Ji, Y. Liu, and Y. Huang, "Cooperative NOMA systems with partial channel state information over Nakagami-*m* fading channels," *IEEE Trans. Commun.*, vol. 66, no. 3, pp. 947–958, Mar. 2018.
[21] X. Li, J. Li, Y. Liu, Z. Ding, and A. Nallanathan, "Outage performance of cooperative NOMA networks with hardware impairments," in *Proc. IEEE Global Commun. Conf. (GLOBECOM)*, Dec. 2018, pp. 1–6.
[22] X. Li, J. Li, P. T. Mathiopoulos, D. Zhang, L. Li, and J. Jin, "Joint impact of hardware impairments and imperfect CSI on cooperative SWIPT NOMA multi-relaying systems," in *Proc. IEEE/CIC Int. Conf. Commun. China (ICCC)*, Aug. 2018, pp. 95–99.
[23] X. Li, J. Li, and L. Li, "Performance analysis of impaired SWIPT NOMA relaying networks over imperfect weibull channels," *IEEE Syst. J.*, to be published.
[24] X. Wang, M. Jia, I. W.-H. Ho, Q. Guo, and F. C. M. Lau, "Exploiting full-duplex two-way relay cooperative non-orthogonal multiple access," *IEEE Trans. Commun.*, vol. 67, no. 4, pp. 2716–2729, Apr. 2019.
[25] Y. Jing and H. Jafarkhani, "Single and multiple relay selection schemes and their achievable diversity orders," *IEEE Trans. Wireless Commun.*, vol. 8, no. 3, pp. 1414–1423, Mar. 2009.
[26] Z. Ding, H. Dai, and H. V. Poor, "Relay selection for cooperative NOMA," *IEEE Wireless Commun. Lett.*, vol. 5, no. 4, pp. 416–419, Aug. 2016.
[27] X. Yue, Y. Liu, S. Kang, A. Nallanathan, and Z. Ding, "Spatially random relay selection for full/half-duplex cooperative NOMA networks," *IEEE Trans. Commun.*, vol. 66, no. 8, pp. 3294–3308, Aug. 2018.
[28] Z. Yang, Z. Ding, Y. Wu, and P. Fan, "Novel relay selection strategies for cooperative NOMA," *IEEE Trans. Veh. Technol.*, vol. 66, no. 11, pp. 10114–10123, Nov. 2017.
[29] P. Xu, Z. Yang, Z. Ding, and Z. Zhang, "Optimal relay selection schemes for cooperative NOMA," *IEEE Trans. Veh. Technol.*, vol. 67, no. 8, pp. 7851–7855, Aug. 2018.
[30] Z. Yu, C. Zhai, J. Liu, and H. Xu, "Cooperative relaying based non-orthogonal multiple access (NOMA) with relay selection," *IEEE Trans. Veh. Technol.*, vol. 67, no. 12, pp. 11606–11618, Dec. 2018.
[31] A. D. Wyner, "The wire-tap channel," *Bell Syst. Tech. J.*, vol. 54, no. 8, pp. 1355–1387, Oct. 1975.
[32] M. Zhang and Y. Liu, "Energy harvesting for physical-layer security in OFDMA networks," *IEEE Trans. Inf. Forensics Security*, vol. 11, no. 1, pp. 154–162, Jan. 2016.
[33] L. Fan, N. Yang, T. Q. Duong, M. Elkashlan, and G. K. Karagiannidis, "Exploiting direct links for physical layer security in multiuser multirelay networks," *IEEE Trans. Wireless Commun.*, vol. 15, no. 6, pp. 3856–3867, Jun. 2016.
[34] B. He, A. Liu, N. Yang, and V. K. N. Lau, "On the design of secure non-orthogonal multiple access systems," *IEEE J. Sel. Areas Commun.*, vol. 35, no. 10, pp. 2196–2206, Oct. 2017.
[35] X. Yue, Y. Liu, Y. Yao, X. Li, R. Liu, and A. Nallanathan, "Secure communications in a unified non-orthogonal multiple access framework," Apr. 2019, *arXiv:1904.01459*. [Online]. Available: https://arxiv.org/abs/1904.01459
[36] Y. Liu, Z. Qin, M. Elkashlan, Y. Gao, and L. Hanzo, "Enhancing the physical layer security of non-orthogonal multiple access in large-scale networks," *IEEE Trans. Wireless Commun.*, vol. 16, no. 3, pp. 1656–1672, Mar. 2017.
[37] H. Zhang, N. Yang, K. Long, M. Pan, G. K. Karagiannidis, and V. C. M. Leung, "Secure communications in NOMA system: Subcarrier assignment and power allocation," *IEEE J. Sel. Areas Commun.*, vol. 36, no. 7, pp. 1441–1452, Jul. 2018.
[38] H. Lei, J. Zhang, K. Park, P. Xu, I. S. Ansari, G. Pan, B. Alomair, and M. Alouini, "On secure NOMA systems with transmit antenna selection schemes," *IEEE Access*, vol. 5, pp. 17450–17464, 2017.
[39] H. Lei, J. Zhang, K.-I. Park, P. Xu, Z. Zhang, G. Pan, and M. Alouini, "Secrecy outage of max–min TAS scheme in MIMO-NOMA systems," *IEEE Trans. Veh. Tech.*, vol. 67, no. 8, pp. 6981–6990, Aug. 2018.
[40] J. Chen, L. Yang, and M.-S. Alouini, "Physical layer security for cooperative NOMA systems," *IEEE Trans. Veh. Technol.*, vol. 67, no. 5, pp. 4645–4649, May 2018.
[41] H. Lei, Z. Yang, K.-H. Park, I. Ansari, Y. Guo, G. Pan, and M.-S. Alouini, "Secrecy outage analysis for cooperative NOMA systems with relay selection scheme," Nov. 2018, *arXiv:1811.03220*. [Online]. Available: https://arxiv.org/abs/1811.03220
[42] F. B. Hildebrand, *Introduction to Numerical Analysis*. New York, NY, USA: Dover, 1987.

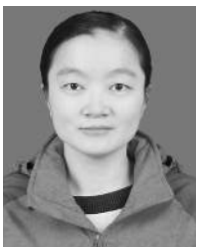

ZHENLING WANG received the B.S. degree from the Information Engineering University of People's Liberation Army, in 2009, and the M.S. degree from Henan Normal University, in 2012. She is currently pursuing the Ph.D. degree with the School of Communication and Information Engineering, Shanghai University.

Her research interests include 5G networks, the Internet of Things, cooperative networks, and non-orthogonal multiple access.

ZHANGYOU PENG received the M.S. degree in communication engineering from Tsinghua University, in 1992, and the Ph.D. degree from Shanghai University, in 2009, where he has been a Professor with the School of Communication and Information Engineering, since 2002.

His research interests include satellite and radar signal processing, weak signal processing, and wireless communication.